Journal of Materials Chemistry B

Accepted Manuscript

ROYAL SOCIETY OF CHEMISTRY

www.rsc.org/materialsB

Carbon Nanotube Uptake Changes the Biomechanical Properties of Human Lung Epithelial Cells in a Time-dependent Manner

*Chenbo Dong#, Reem Eldawud#, Linda M. Sargent, Michael L. Kashon, David Lowry, Yon Rojanasakul, and Cerasela Zoica Dinu**

C. Dong, R. Eldawud, Prof. C. Z. Dinu
Department of Chemical Engineering,
West Virginia University
Morgantown WV, 26506, USA
E-mail: cerasela-zoica.dinu@mail.wvu.edu

Dr. L. M. Sargent, Dr. M. L. Kashon, D. L. Lowry,
National Institute for Occupational Safety and Health
Morgantown WV, 26505, USA

Prof. Y. Rojanasakul
Department of Basic Pharmaceutical Sciences
West Virginia University
Morgantown WV, 26506, USA

# Equally contributing authors
* Corresponding author

Abstract

The toxicity of engineered nanomaterials in biological systems depends on both the nanomaterial properties and the exposure duration. Herein we used a multi-tier strategy to investigate the relationship between user-characterized multi-walled carbon nanotubes (MWCNTs) exposure duration and their induced biochemical and biomechanical effects on model human lung epithelial cells (BEAS-2B). Our results showed that exposure to MWCNTs leads to time-dependent intracellular uptake and generation of reactive oxygen species (ROS), along with time-dependent gradual changes in cellular biomechanical properties. In particular, the amount of internalized MWCNTs followed a sigmoidal curve with the majority of the MWCNTs being internalized within 6 h of exposure; further, the sigmoidal uptake correlated with the changes in the oxidative levels and cellular biomechanical properties respectively. Our study provides new insights into the time-dependent induced toxicity caused by exposure to occupationally relevant doses of MWCNTs and could potentially help establish bases for early risk assessments of other nanomaterials toxicological profiles.

Introduction

The versatility in physical and chemical properties including high strength to weight ratio,[1, 2, 3] electrical[4] and thermal conductivity[5] make multi-walled carbon nanotubes (MWCNTs) attractive candidates for applications in a wide variety of fields from electronic devices,[6] sports equipment,[7] aerospace industry,[8] to sensors[9] and composite materials.[10] Recently, functionalization of MWCNTs with amino acids,[11] peptides,[12] and other small biomolecules[13] has been explored for biomedical and biotechnological applications in gene[14] and drug delivery,[15] bioimaging,[16] and for therapeutics.[17] However, as the list of potential bio-related applications increases, so do concerns regarding MWCNTs potential to induce toxicity in biological systems.[18]

Studies showed that MWCNTs interactions with biological systems are dependent on the nanomaterial physico-chemical properties, with MWCNT-induced toxicity being attributed to various material's characteristics including size,[19] surface charge,[20] and aggregation state.[21] Studies also revealed that upon uptake through either piercing[22] or endocytosis,[23] MWCNTs translocate the cell altering its physiological properties and fate, by causing cyto and genotoxicity. For instance, research showed that MWCNTs cytoplasmic translocation resulted in reactive oxygen species (ROS) generation[24, 25] and changes in cellular elasticity,[26] with variations in the cellular mechanical properties indicating cellular transformation and potential for cancer development.[26-28] Further analysis showed that MWCNTs containing precursor metal catalysts displayed a stronger toxicity than their catalyst-free counterparts.[29] Reduced toxicity was observed upon acid washing and carboxylation of MWCNTs,[30] with the diminished effects being attributed to the nanotube shorter lengths and higher dispersity resulted from acid cutting at the MWCNT defect sites, as well as grafting of O-related functionalities.[31] For genotoxicity, uptake of MWCNTs resulted in their initial accumulation in the cell endosome[32]; subsequent release in the cytoplasm led to MWCNT interactions with cell nucleus,[23] polyploidy,[33] changes in chromosome numbers,[34] and disruption of mitosis,[35] just to name a few.

Based on these previous studies showing that MWCNTs uptake and cellular translocation result in complex interactions with cellular components, we now begin to understand how exposure to nanotubes may be involved in the mechanisms responsible of cancer initiation.[36] However, predicting the time of uptake in relation to the nanomaterial physico-chemical properties and its aggregation state, as well as predicting time-dependent nanotube-induced cellular fate upon nanomaterial internalization have been challenging. Further, the correlations between early onsets of exposure and immediate cellular responses are still lacking. Assessment of early exposure onsets are required for preventing MWCNT-induced deleterious effects, to reduce the risks for cell transformation or cancer development[28, 34, 36] to thus help contribute to the next generation of biomedical applications or products based on these nanomaterials.[37]

The present study aimed to investigate the cellular effects induced by short duration (1-12 h) exposure to occupational relevant doses of MWCNTs as derived from recommendations made by the Occupational Safety and Health Administration (OSHA) for particles less than 5 μm in diameter.[28] By using a combination of analytical techniques relying on Fluorescence Activated Cell Sorting (FACS), Atomic Force Microscopy (AFM) nanoindentation and a versatile human lung epithelial cells (BEAS-2B) model,[26, 28] we assessed MWCNT-induced cellular changes and investigated how early cellular uptake and MWCNT cytoplasmic accumulation lead to biomechanical and biochemical cell transformations and thus help explain cellular fate as well as to possibly set norms for onsets risk assessment of this nanomaterial.

Materials and Methods

Multi-Walled Carbon Nanotubes (MWCNTs) washing

Commercial multi-walled carbon nanotubes (MWCNTs; 95% purity, PD15L5-20, 10-20 nm in diameter, 1-5 μm in length) purchased from Nanolab Inc. were washed in a mixture of 3:1 (V/V) concentrated sulfuric (96.4%, Fisher, USA) and nitric (69.5%, Fisher, USA) acids using established protocols.[31] Briefly, the MWCNT-acids mixture was sonicated in an ice bath sonicator (Branson 2510, Fisher, USA) at a temperature lower than 23°C for 1 h. Subsequently, the mixture was diluted in deionized (di) water (2 L), and filtered through a GTTP 0.2 μm polycarbonate filter membrane (Millipore, Fisher, USA). The acid washed MWCNTs (simply called MWCNTs) isolated on the filter membrane were subsequently redispersed in di water; filtration cycles were repeated at least 3 other times to remove acid traces and any released impurities or dissociated catalysts. The nanotubes isolated on the filter membrane were subsequently dried in a vacuum desiccator and stored at room temperature until further use.

Characterization of MWCNTs

A combination of analytical techniques was employed to determine MWCNT physical and chemical properties. Briefly, Energy Dispersive X-Ray spectroscopy (EDX) was used to investigate the elemental composition of the MWCNTs; the analysis was performed on a Hitachi S-4700 Field Emission Scanning Electron Microscope (USA) combining secondary (SE) and backscattered (BSE) electron detection, and operating in a single unit at 20 kV.

Dispersity of MWCNTs was evaluated by suspending MWCNT samples in three different dispersing agents, i.e. di water, phosphate buffer (PBS, pH=7.4, Invitrogen, USA) and Dulbecco's Modified Eagle Media (DMEM, Invitrogen, USA) with or without 10% Fetal Bovine Serum (FBS, Invitrogen, USA). The corresponding solutions (3 mg/ml of sample) were centrifuged at 3000 rpm for 5 min; subsequently, 0.8 mL of each of the supernatant was removed and filtered through a 0.2 μm GTTP membrane. The sample isolated on the filter membrane was dried under vacuum and the amount of MWCNTs retained on the filter was weighed. The sample dispersity was calculated in relation to the starting volume and amount of dry MWCNTs on the filter membrane.

The length distribution of MWCNTs was evaluated using an Atomic Force Microscope (AFM) with Si tips operating in air and in tapping mode (Asylum Research, AC240TS, 50 to 90 kHz). The average length of the MWCNT samples was evaluated by investigating the length of 30 individual MWCNTs from 3 areas, each of 10 μm × 10 μm.

A Renishaw InVia Raman Spectrometer (CL532-100, 100 mW, USA) was used to investigate MWCNT chemical structure. Briefly, 1 mg of sample was mounted onto clean glass substrates (Fisher, USA) and irradiated using an argon ion (Ar^+) laser beam operating at 514.5 nm and having a spot size below 0.01 mm^2. To reduce sample heating effects the exposure time was kept at 10 sec; the scan range was set between 100 and 3200 cm^{-1}.

Generation of MWCNT-based conjugates

Alexa 488 Bovine Serum Albumin 488 (Alexa-BSA; Sigma, USA) was covalently immobilized onto MWCNTs using 1-ethyl-3-[3-dimethylaminopropyl] carbodiimide hydrochloride (EDC, Acros Organics, USA) and N-hydroxysuccinimide (NHS, Pierce, USA) chemistry.[31, 38, 39] Briefly, 2 mg of MWCNTs were dispersed in 160 mM EDC and 80 mM NHS

(total volume of 2 mL) in (2-N-morpholino) ethanesulfonic acid sodium salt (MES buffer, 50 mM, pH 4.7, Sigma, USA) for 15 min at room temperature on a bench shaker operating at 200 rpm. EDC/NHS activated MWCNTs were subsequently filtered through a 0.2 μm GTTP filter membrane, washed thoroughly with MES buffer to remove ester residues, and immediately re-dispersed in 2 mL of 1 mg/mL Alexa-BSA solution in PBS, pH 7.4 for 3 h at room temperature with shaking at 200 rpm. When the time elapsed, the resulting Alexa-BSA-MWCNT conjugates were filtered and washed extensively with PBS to remove any unbound protein. The supernatant and the first two washes were collected to help quantify the amount of protein washed out (i.e., amount of protein not bound to the MWCNTs).

Protein loading onto MWCNTs

The amount of Alexa-BSA immobilized onto MWCNTs (i.e., loaded protein) was determined using standard colorimetric bicinchoninic acid assay (BCA , Pierce, USA) by subtracting the amount of protein washed out in the supernatant and the first two washes from the amount of protein offered to the MWCNTs during the initial incubation step. Briefly, the working reagent was prepared by mixing 50 parts of reagent A (1000 μL), with 1 part of reagent B (20 μL). Next, 1000 μl of the working reagent was mixed with 50 μL of the supernatant or the isolated washes. The resulting solution was vortexed lightly and incubated in a water bath at 37^{o}C for 30 min. Subsequently, the sample absorbance was monitored at 562 nm (Spectrophotometer, Evolution 300/600, Thermo Fisher, USA) and compared to the absorbance of known concentrations of free Alexa-BSA in PBS mixed with the working buffer.

Emission efficiency of the loaded protein

The emission efficiency of the Alexa-BSA loaded onto the MWCNTs surface was evaluated using a spectroscopical assay.[38, 40] Briefly, the absorbance spectrum of 100 μg/ml of Alexa-BSA-MWCNT conjugates was recorded relative to both the absorbance spectrum of unlabeled MWCNTs (100 μg/ml) and the absorbance spectrum of free Alexa-BSA at an amount equivalent to the amount loaded onto the MWCNTs. The absorbance spectrum of immobilized Alexa-BSA (excitation at 488 nm and emission at 515 nm) was quantified by subtracting the values of the unlabeled MWCNTs from the absorbance values of the Alexa-BSA-MWCNTs, with the efficiency of emission being determined as the height of the absorbance peaks of the bound protein relative to the height of the peaks of free protein in solution.

Cell culture

Human bronchial epithelial cells (BEAS-2B, ATCC, USA) were cultured in DMEM media supplemented with 10% FBS, 2 mM L-glutamine and 100-units/ml penicillin/streptomycin (reagents were purchased from Invitrogen, USA). Cells were passaged regularly using 0.25% (w/v) trypsin (Invitrogen, USA) with 1.5 mM EDTA (Molecular Probes, USA) and maintained in a humidified atmosphere at 37ºC and under 5% CO_2.

Fluorescence Activated Cell Sorting (FACS) analysis

Cells in DMEM media with 10% FBS were seeded in T75 flasks (Fisher, USA) for 24 h at a density of 3.71 x 10^5 cells and subsequently treated with 24 μg/cm^2 Alexa-BSA-MWCNT conjugates or unlabeled MWCNTs, each dispersed using a brief bath sonication (5 sec in 1 sec increments) in fresh media. Cellular exposure was performed for different time periods, i.e., 1, 3, 6 or 12 h respectively; control samples of untreated cells or cells exposed to free Alexa-BSA at an equivalent amount to the amount loaded onto the MWCNTs were also performed.

For uptake analysis, cells were washed with fresh PBS, collected using 0.25% trypsin, suspended in DMEM with 10% FBS and centrifuged at 1200 for 5 min to remove non-internalized or loosely bound Alexa-BSA-MWCNT conjugates, free MWCNTs or free Alexa-BSA in solution respectively. Subsequently the samples were washed with PBS, pelleted, and incubated at room temperature for 15 min in 100 µL of glutaraldehyde solution (4%, Sigma, USA). Upon incubation, the samples were washed again with PBS and analyzed using a FACS Caliber flow cytometer (Becton Dickinson, USA). The forward scatter (FSC) and side scatter (SSC) were adjusted using control cells to lay in a range of 0-1000; gating included the majority of the live cell population. FITC signal for the Alexa-BSA or derivate MWCNT-based conjugates used excitation at 488 nm and emission at 515 nm. At least 10000 events were contained in the gated area and data was analyzed and plotted using Flow Jo v7.2.5 software.

Reactive oxygen species (ROS) evaluation

Intracellular ROS generation was determined using the oxidation-sensitive fluorescent probe 2′,7′-dichlorofluorescein diacetate (DCF-DA; Sigma, USA). Upon formation of ROS, cellular esterase hydrolyzes DCF-DA to the highly fluorescent 2', 7'–dichlorofluorescein (DCF).[41] Briefly, BEAS-2B cells were seeded overnight in a 96-well plate (Corning, USA) at a density of $1.5x10^4$ cell per well, and incubated with 5 µM DCF-DA at 37 °C for 30 min. Subsequently, the cells were treated with 24 µg/cm^2 MWCNTs suspended in Hank's Balanced Salt Solution (HBSS; Life Technologies, USA) for different time periods. Control samples of unexposed cells or cells exposed to pristine MWCNTs were also investigated. Quantification of the intracellular levels of ROS was performed using a multi-well plate reader (FLUOstar OPTIMA, BMG LABTECH Inc., USA) and evaluating the DCF fluorescence at 485 nm excitation and 520 nm emission respectively.

Biomechanical analysis

Cells were seeded at a density of 10^5 cells in 50 mm x 9 mm petri dishes (BD Biosciences, USA) and exposed to 24 µg/cm^2 of MWCNTs for 1, 3, 6 or 12 h, respectively. The exposed cells were washed twice with PBS (5 min for each washing step) and fixed with 4% glutaraldehyde solution for 30 min. Three additional washing steps were performed to remove free glutaraldehyde; the petri dishes were subsequently filled with PBS and used for elasticity analysis. Elastic modulus analysis of the BEAS-2B cells exposed to MWCNTs or of the unexposed control cells were performed using an AFM integrated with an inverted fluorescence microscope (MFP-3D-BIO AFM, Asylum Research, USA). The nanomechanical properties of control cells and cells exposed to MWCNTs were evaluated using Sneddon's modification of the Hertz model developed for a four-sided pyramid.[42-44] Force-displacement curves acquired during elastic mapping were converted into force-indentation curves[45] based on the assumption that the indentation depth of the sample is extremely thick.[46] The cells elasticity (Young's modules, E) was evaluated knowing the indentation of the tip, δ, the Poisson's ratio v for the cell (0.5 [44]) and the opening angle of the tip, i.e., α=36°. The cantilever was calibrated against a plastic substrate and its exact spring constant was determined using thermal tuning method prior every experiment.[47] The trigger force was in the nanonewtons range (i.e., 2.8-4.6 nN) and the fitting percentage used for all experiments analysis was 90%.

Statistical analysis

Alexa-BSA loading onto the MWCNTs and Alexa-BSA functionality analysis were repeated six times. FACS experiments were performed in triplicates and repeated three times. The triplicate samples were averaged to provide three independent replications. ROS experiments were performed for four independent replicates and repeated three times; for a total of minimum 12 samples per each time point. All results are presented as mean ± standard deviation. Two-way analysis of variance (ANOVA) and unpaired two-tailed Student's T-test were performed using JMP 8.0 (SAS Institute) and Sigma Plot 10.0 (Systat Software Inc.). The elasticity experiments were performed using a complete randomized block design with each block containing two cell culture dishes; three independent blocks were run for each one of the experimental onsets being investigated. For each culture, six individual randomly selected cells were examined for the biomechanical analysis and averaged into a single value as cells from the same culture are not independent. The variables were analyzed using the Proc Mixed procedure in SAS/Stat for Windows (SAS) with experimental block modeled as a random effect.

All differences were considered statistically significant for $p^* < 0.05$.

Results and Discussion

A multi-tier strategy was used to investigate the cellular responses to differential uptake of user-characterized multi-walled carbon nanotubes (MWCNTs). The strategy involved time-controlled exposures of model human lung epithelial cells (BEAS-2B)[26, 28] to occupationally relevant doses of 24 μg/cm^2 of MWCNTs with user-characterized physical and chemical properties. The exposure dose chosen for this investigation was based on previous recommendations made by the Occupational Safety and Health Administration (OSHA) for particles less than 5 μm in diameter; [28] the dose corresponds to human work space exposure of 8 years at 5 mg/m^3 and was extrapolated from *in vivo* CNT exposure data normalized to alveolar surface area of mice lungs.[28, 34, 48] The proposed multi-tier strategy is aimed to help identify the early exposure onsets-induced cellular fate and potential deleterious effects of MWCNTs thus further our understanding of nanotube-induced toxicity.

The physical and chemical properties of MWCNTs were determined using energy dispersive X-ray spectroscopy (EDX) for elemental composition and Atomic Force Microscopy (AFM) for nanotubes length. Previous studies have shown that the presence of high contents of metal impurities (Fe and Ni) in nanotubes could induce mitochondrial membrane damage, generation of reactive oxygen species (ROS), loss in intracellular low molecular weight thiols (GSH) and accumulation of lipid hydroperoxides macrophages.[36, 37, 49] Our analysis revealed that the MWCNTs used in this study had minimum traces of Fe and Cu catalysts (combined, only about 1.50 wt%), with the dominant element being carbon (C, 90.25 wt%; Table S1). The presence of oxygen (O, 7.56 wt%) in the sample was presumably due the washing of the pristine (as purchased) MWCNTs in the mixture of sulfuric and nitric acids known to graft O-related functional groups.[31] Such grafting was further responsible for the observed increased dispersity of the nanotubes in different media, all relative to their pristine counterparts (Table S2). Lastly, ~75% of nanotube shortening was observed by AFM analysis (i.e., 1040±553 nm from 4261±2354 nm respectively) confirming previous reports (Table S3).[26, 50]

Fluorescence Activated Cell Sorting (FACS) was used to evaluate the uptake of the user-characterized MWCNTs.[36, 51] For this MWCNTs were covalently functionalized with 488 Alexa Bovine Serum Albumin (Alexa-BSA) using the O-related functional groups grafted upon acid

treatment and a zero-length chemistry;[52] covalent immobilization of the Alexa-BSA ensured stable protein binding thus eliminating concerns associated with possible protein removal during MWCNTs sonication in cellular media. Alexa-BSA labeling was the preferred method to facilitate FACS analysis of MWCNTs uptake since previous studies showed that the protein does not significantly change the internalization conditions of the nanotubes, with *in vitro* studies assessing and comparing cellular-induced fate upon exposure to both labeled or unlabeled nanotubes present in media enriched with free amino acids, nutrition factors and BSA.[53, 54]

Our loading analysis showed that the amount of Alexa-BSA immobilized onto the MWCNTs was 0.22 ±0.06 mg protein per mg MWCNTs, comparable to previous published reports.[55-57] Our dispersity analysis (Table S2) comparing labeled and unlabeled MWCNTs dispersed in cellular media (the cellular media contains free protein and amino acids, with a minimum of 1 mg/ml glucose, 7.6 mg/ml proteins and 4.6 mg/ml albumins respectively[58, 59]) did not reveal significant changes in the sample dispersity, all relative to control buffer systems, while spectroscopy analysis confirmed that the immobilized Alexa-BSA retained its functionality. In particular, the efficiency of fluorescence emission of the immobilized protein relative to the free protein in solution at the same amount was 34 ± 9% (Figure 1a); the reduced efficiency was presumably due to the protein deformation and quenching at the nanotube interface.[38, 39] Raman spectroscopy also confirmed protein immobilization as a change in the I_D/I_G ratio of Alexa-BSA-MWCNTs (0.967) relative to MWCNTs alone (0.799) (Figure 1b, Table S4) where the I_D/I_G represents the degree of disorder in the C-based structure with the G band being related to the presence of sp2 species[60] and the D band being associated with defects and non-crystal species.[61]

The change in the fluorescence intensity of the cells exposed to Alexa-BSA-MWCNT conjugates relative to controls (i.e., unexposed cells, cells exposed to the same amount of free Alexa-BSA as the amount additionally loaded onto the nanotubes, or cells exposed to MWCNTs) as recorded by FACS is shown in Figure 2. The analysis showed that within the first hour of exposure (Figure 2a), the uptake of Alexa-BSA-MWCNTs was relatively slow and did not result in significant changes in the FITC signal of the exposed cells relative to their controls. A higher FITC signal was however observed upon cellular uptake of the free Alexa-BSA; this was presumably associated with the free protein's ability to cross the cellular membrane more efficiently than its MWCNT-immobilized counterpart.[62] Analysis also showed that longer exposure time led to a gradual increase in the FITC signal of the cells exposed to Alexa-BSA-MWCNT conjugates and free Alexa-BSA respectively, both relative to unexposed cells or cells exposed to MWCNTs (Figure 2a). Specifically, after 3 h of exposure there was a 55% increase in the FITC signal of the cells exposed to Alexa-BSA-MWCNTs relative to unexposed cells, a 19% increase relative to cells exposed to unlabeled MWCNTs, and a 12% increase relative to cells exposed to free Alexa-BSA. Similarly, after 6 h of exposure, the FITC signal of the cells exposed to Alexa-BSA-MWCNTs showed a 92%, 50%, and 20% change relative to the FITC signal of the unexposed cells, cells exposed to unlabeled MWCNTs, or cells exposed to free Alexa-BSA respectively. Finally, after 12 h exposure the FITC signal of the cells exposed to Alexa-BSA-MWCNTs was about 100% higher than that of the unexposed cells and cells exposed to unlabeled MWCNTs respectively, and only slightly higher (not statistically significant) than that of the cells exposed to free Alexa-BSA.

The lower FITC signal observed for the cells exposed to free Alexa-BSA relative to the cells exposed to the Alexa-BSA-MWCNT conjugates is presumably due to increased free protein susceptibility for proteosomal degradation[63] relative to its immobilized counterpart known to

have increased stability upon immobilization at the MWCNTs interface.[38] Although the signal of cells exposed to unlabeled MWCNTs did not yield significant differences relative to unexposed cells at all the time points being investigated, it seemed to have gradually increased with the exposure duration up to 6 h only to return to its baseline after 12 h. Such trend is presumably associated with increased MWCNTs intracellular translocation, association and co-localization with cellular elements[35, 64] that will interfere with the intrinsic fluorescence of the MWCNTs to thus lead to the observed change in intensity.[36, 65, 66]

Figure 2b shows the comparative cross-analysis of the normalized fluorescent intensity of the cells exposed to Alexa-BSA-MWCNT conjugates relative to unexposed cells, all as a function of the exposure time. The analysis showed that the uptake of Alexa-BSA-MWCNT conjugates followed a three parameter sigmoid curve and increased with the exposure time. Specifically, within the first hour of exposure there was a 15% increase in the fluorescent intensity, while between 1 and 3 h of exposure the fluorescent intensity of cells exposed to the conjugates increased by 39% accounting for a total increase of ~54% in 3 h time frame, all relative to the intensity of unexposed control cells. Furthermore, between 3 and 6 h of exposure there was an additional 37% increase in the fluorescence intensity, while between 6 and 12 h the increase in intensity was less evident. These results are in agreement with previous reports that showed that the highest increase in CNTs cellular uptake and internalization occur within 3 h from initial cellular exposure.[32, 67]

We correlated the differential, time-dependent uptake as recorded by FACS with the intracellular oxidative species (ROS) using 2',7'-dichlorofluorescein diacetate (DCF-DA) fluorescence probe.[68] Our aim was to determine whether the observed time-dependent, differential uptake leads to a gradual formation and accumulation of ROS; the interest in ROS is driven by the current research which shows that superoxide (O^{2-}), hydroxyl radical (OH^{-}), and nonradical derivatives of O such as hydrogen peroxide (H_2O_2) accelerate cell death by damaging cellular components including DNA, proteins, and lipid membranes.[69-72] ROS generation following MWCNTs exposure was previously shown to lead to changes in the mitochondrial potential and apoptosis signaling activation,[71, 73] with ROS generation depending of acellular factors such as particle surface, size, composition and/or being due to cellular responses resulting from MWCNTs-cell interaction.

Our ROS analysis complemented FACS results and showed increased levels in the amount of ROS generated following 1, 3 and 6 h exposure to MWCNT and decreased levels similar to those of controls after 12 h of exposure (Figure 3). The significant increase in the ROS after 1 h exposure is associated with the high sensitivity of the DCF-DA fluorescent probe which can record O_2, OH^{-}, or H_2O_2 at very low concentrations even after a reduced uptake of the nanotubes; this is in contrast with the FACS sensitivity which requires higher FITC signal for detection.[74] The drop after 12 h of exposure is presumably associated either with the regulations in the intracellular glutathione (GSH), a major antioxidant that protects cells from oxidative stress[75] or the quenching effects of the internalized MWCNTs.[76] In particular, prolonged MWCNTs exposure could lead to a gradual accumulation of GSH which will eventually balance the cellular ROS oxidative levels.[77, 78] Complementary, intracellular accumulation of MWCNTs could lead to quenching of the cell-derived radicals by scavenging of the oxygen-centered molecules (i.e., HO^{-} and O_3^{+}).[79] Controlled experiments of the ROS levels of the cells exposed to purified MWCNTs relative to pristine counterparts are also shown (Supporting information, Figure S1). Results showed that the ROS levels for the cells exposed to pristine MWCNTs followed a similar trend to that of the cells exposed to their purified counterparts. The ROS

levels for the cells exposed to pristine MWCNTs was significantly higher than that of control cells within the first hour of exposure, reached a maximum value after aproximatly 8 h of exposure and eventually decreased with time remaining yet significantly higher than controls even after longer exposure duration (i.e., 12 h). Cross-comparision of the ROS levels between the cells exposed to pristine and purified MWCNTs respectively, showed that the pristine samples induced significantly higher ROS levels relative to their purified counterparts, for all time points being investigated. This observation is presumably associated either with the larger aspect-ratio of the pristine MWCNTs (as confirmed by AFM), their increased levels of metal impurities, (i.e., Fe[49, 73, 80, 81]; as confirmed by our EDX analysis), and/or lower dispersity (see dispersity analysis; Table S2).

Based on these results which showed both differential, time-dependent uptake and intracellular ROS generation upon cells exposure to MWCNT, we hypothesize that MWCNTs accumulation in the cell leads to changes in cellular biomechanics, all in a time-dependent manner. Our hypothesis is supported by previous studies which showed that cells exposed to iron-based nanoparticles generate ROS which induces changes in their cytoskeleton and mechanical properties[82] as well as our own previous studies which showed that exposure to MWCNTs for a determined time frame of 24 h induce changes in cellular biomechanics with nanotubes localization at the cell nucleus.[26]

The degree of cellular biomechanical changes upon 1, 3, 6 or 12 h of cellular exposure to MWCNTs were investigated using AFM and nanoindentation.[26] Specifically, micro-scale cellular stiffness was assessed from the bending of the AFM cantilever upon tip indentation in response to a known applied force; fitting the force-indentation curve to the Hertz model provided quantitative measurements of both the cell body as well as cell nucleus as distinguished based on the interactions between the AFM tip and the cell.[36] In particular, nuclear regions are known to show weaker engaging of the AFM tip than the cell edges due to their less concentrated cytoskeleton fibers as well as higher height above the surface.[36, 83]

Analysis of the BEAS-2B cells exposed to MWCNTs for 1, 3, 6 or 12 h and fixed with glutaraldehyde is shown in Figure 4; the fixation was chosen as a mean to preserve the cellular properties during tip scanning.[26] Results indicated that control cells have Young's modulus ranging from 100 to 400 kPa with higher values recorded at the cell periphery (> 600 kPa) presumably due to the underlying plastic substrate. The nuclear region appeared softer when compared to the cellular body, showing Young's modulus values between 20-200 (Figure 4a). The elastic modulus for both control and exposed cells was about one magnitude higher than those of the live cells[83, 84] presumably due to the experimental conditions being used (i.e., glutaraldehyde fixation[84] and/or AFM indentation approach performed at low speed).[85]

The average Young's modulus of unexposed cells and cells exposed to MWCNTs for different onsets are shown in Figure 4b (whole cell) and 4c (cell nucleus) respectively. Analysis showed that 1 and 3 h exposures did not result in significant changes in the elastic moduli of the whole cells being studied however, 3 h exposure lead to significant changes in the Young's modulus of the nuclear regions of the exposed cells relative to their control counterparts. For longer exposure (>6 h), the elastic moduli of exposed cells (both whole cells and cells nuclei) showed a significant increase relative to their controls at the corresponding time points ($p^* < 0.05$), presumably because of the larger cellular accumulation of the uptaken nanotubes.[32] Specially, after 6 h, exposed cells showed an increase of about 39% and 49% of their whole and nuclear Young's modulus respectively relative to their counterparts, i.e., unexposed cells. At 12 h, exposed cells also showed an increase in their overall Young's modulus of about 22% and an

increase of 28 % in their nuclei Young's moduli both relative to their control counterparts. Such increases in Young modulus were significant and presumably due to the interactions of uptaken MWCNTs with cytoskeleton filaments like actin[86] or microtubules,[35] or the DNA.[72]

The current study contributes to advancing understanding of both biochemical and biomechanical cellular transformations upon exposure to MWCNTs with our analysis showing that early-induced cellular responses could be considered/have the potential to become adverse. In particular, our results emphasize the importance of studying the MWCNT-induced cell transformations at early onsets to understand the fundamental interactions of the uptaken MWCNTs with the cellular components, their cellular translocation and overall influence on the cellular fate. With the known affinity of the internalized MWCNTs for cytoskeletal elements,[28, 35, 87] and cellular biomechanics ability to regulate homeostasis, cell proliferation, motility, and differentiation,[88-90] subtle changes in the cellular mechanical properties can be correlated with phenotypical transformation and cancer initiation.[91] While to our knowledge no previous studies have reported biomechanical cellular changes induced by exposure to MWCNTs at early onsets, our study is supported by a previous one showing that 24 h of exposure to MWCNTs induce changes in cellular biomechanics with nanotubes localization at the cell nucleus resulting in potential cell transformation to a malignant phenotype.[26] The differential, time-dependent mechanical changes observed upon early onsets cellular exposure could thus help prevent MWCNT-induced deleterious effects by reducing the risks for cell transformation.[28, 34, 36]

Further, our studies stress that in order to circumvent deleterious effects associated with nanomaterials exposure and to advance MWCNTs implementation in biomedical applications, one not only has to tightly control the exposure time but further to evaluate cellular changes and cellular ability to regain its homeostasis and how such processes are related to the differential time-dependent exposure. In particular, it is expected that assessment of early onsets of exposure derived from such studies would lead to more protective measurements than those based on direct adverse effects. For instance, such an assessment could provide a secondary level of prevention when exposure to MWCNTs is being considered;[92] by helping identify and distinguish early on the possible reactivities of the nanomaterials, methods to minimize their induced risks early in their design or manufacturing and down-stream user processes could be established.

Conclusions

The present study showed that exposure of human lung epithelial cells to occupationally relevant doses of user-characterized MWCNTs leads to their time-differential uptake, and induced ROS generation and biomechanical cellular changes. In particular, our study showed that most of the MWCNTs uptake occurred within 6 h of cellular exposure. Furthermore, our results showed that 3 h exposure leads to changes in the cell elastic properties with further changes in the overall biomechanical properties being gradual and dependent on the exposure time. Assessment of the biomechanical properties of the exposed cells and their changes in elasticity suggest the ability to determine the underlying basis for MWCNT-induced cell transformation and toxicity using *in vitro* model cellular systems.

Acknowledgements

This work was supported by National Science Foundation (NSF) grant EPS-1003907, NSF 1434503, NORA 927000Y, and the National Institute of Health (NIH; R01-ES022968). The

authors acknowledge use of WVU Shared Research Facilities, WVU Flow Cytometry Core Facility (Supported by National Institute of Health equipment grant number S10OD016165 and the Institutional Development Award (IDeA) from the National Institute of General Medical Sciences of the National Institutes of Health under grant numbers P30GM103488 (CoBRE) and P20GM103434 (INBRE)). Authors also acknowledge the support and expertise of Dr. Karen Martin, the director of the Core Facility, and help of Jeremy Hardinger with EDX analysis.

Conflict of Interests

Research findings and conclusions are those of the authors and do not necessarily represent the views of the National Institute for Occupational Safety and Health. The authors declare no competing financial interest.

References

1. X. F. Zhang, Q. W. Li, T. G. Holesinger, P. N. Arendt, J. Y. Huang, P. D. Kirven, T. G. Clapp, R. F. DePaula, X. Z. Liao, Y. H. Zhao, L. X. Zheng, D. E. Peterson and Y. T. Zhu, *Adv Mater*, 2007, 19, 4198-+.
2. B. G. Demczyk, Y. M. Wang, J. Cumings, M. Hetman, W. Han, A. Zettl and R. O. Ritchie, *Mat Sci Eng a-Struct*, 2002, 334, 173-178.
3. J. H. Zou, J. H. Liu, A. S. Karakoti, A. Kumar, D. Joung, Q. A. Li, S. I. Khondaker, S. Seal and L. Zhai, *Acs Nano*, 2010, 4, 7293-7302.
4. I. Stavarache, A. M. Lepadatu, V. S. Teodorescu, M. L. Ciurea, V. Iancu, M. Dragoman, G. Konstantinidis and R. Buiculescu, *Nanoscale Res Lett*, 2011, 6.
5. A. E. Aliev, M. H. Lima, E. M. Silverman and R. H. Baughman, *Nanotechnology*, 2010, 21.
6. S. W. Lee, B. S. Kim, S. Chen, Y. Shao-Horn and P. T. Hammond, *J Am Chem Soc*, 2009, 131, 671-679.
7. M. F. L. De Volder, S. H. Tawfick, R. H. Baughman and A. J. Hart, *Science*, 2013, 339, 535-539.
8. O. Gohardani, M. C. Elola and C. Elizetxea, *Progress in Aerospace Sciences*, 2014, 70, 42-68.
9. S. Dhall, N. Jaggi and R. Nathawat, *Sensor Actuat a-Phys*, 2013, 201, 321-327.
10. K. Woan, G. Pyrgiotakis and W. Sigmund, *Adv Mater*, 2009, 21, 2233-2239.
11. S. Mallakpour and A. Zadehnazari, *Synthetic Met*, 2013, 169, 1-11.
12. M. S. Deshpande and S. Mazumdar, *Biomacromolecules*, 2012, 13, 1410-1419.
13. M. Gasser, B. Rothen-Rutishauser, H. F. Krug, P. Gehr, M. Nelle, B. Yan and P. Wick, *J Nanobiotechnol*, 2010, 8.
14. K. Bates and K. Kostarelos, *Adv Drug Deliver Rev*, 2013, 65, 2023-2033.
15. S. Y. Madani, N. Naderi, O. Dissanayake, A. Tan and A. M. Seifalian, *Int J Nanomed*, 2011, 6, 2963-2979.
16. J. J. Khandare, A. Jalota-Badhwar, S. D. Satavalekar, S. G. Bhansali, N. D. Aher, F. Kharas and S. S. Banerjee, *Nanoscale*, 2012, 4, 837-844.
17. H. Ali-Boucetta, K. T. Al-Jamal, D. McCarthy, M. Prato, A. Bianco and K. Kostarelos, *Chem Commun*, 2008, DOI: Doi 10.1039/B712350g, 459-461.
18. D. W. Porter, A. F. Hubbs, R. R. Mercer, N. Q. Wu, M. G. Wolfarth, K. Sriram, S. Leonard, L. Battelli, D. Schwegler-Berry, S. Friend, M. Andrew, B. T. Chen, S. Tsuruoka, M. Endo and V. Castranova, *Toxicology*, 2010, 269, 136-147.
19. S. K. Sohaebuddin, P. T. Thevenot, D. Baker, J. W. Eaton and L. P. Tang, *Part Fibre Toxicol*, 2010, 7.
20. R. B. Li, X. Wang, Z. X. Ji, B. B. Sun, H. Y. Zhang, C. H. Chang, S. J. Lin, H. Meng, Y. P. Liao, M. Y. Wang, Z. X. Li, A. A. Hwang, T. B. Song, R. Xu, Y. Yang, J. I. Zink, A. E. Nel and T. Xia, *Acs Nano*, 2013, 7, 2352-2368.
21. Y. Taquahashi, Y. Ogawa, A. Takagi, M. Tsuji, K. Morita and J. Kanno, *J Toxicol Sci*, 2013, 38, 619-628.
22. H. Nagai, Y. Okazaki, S. H. Chew, N. Misawa, Y. Yamashita, S. Akatsuka, T. Ishihara, K. Yamashita, Y. Yoshikawa, H. Yasui, L. Jiang, H. Ohara, T. Takahashi, G. Ichihara, K. Kostarelos, Y. Miyata, H. Shinohara and S. Toyokuni, *P Natl Acad Sci USA*, 2011, 108, E1330-E1338.

23. Q. X. Mu, D. L. Broughton and B. Yan, *Nano Lett*, 2009, 9, 4370-4375.
24. S.-F. Ye, Y.-H. Wu, Z.-Q. Hou and Q.-Q. Zhang, *Biochemical and Biophysical Research Communications*, 2009, 379, 643-648.
25. D. van Berlo, V. Wilhelmi, A. W. Boots, M. Hullmann, T. A. Kuhlbusch, A. Bast, R. P. Schins and C. Albrecht, *Archives of toxicology*, 2014, 88, 1725-1737.
26. C. B. Dong, M. L. Kashon, D. Lowry, J. S. Dordick, S. H. Reynolds, Y. Rojanasakul, L. M. Sargent and C. Z. Dinu, *Adv Healthc Mater*, 2013, 2, 945-951.
27. M. Plodinec, M. Loparic, C. A. Monnier, E. C. Obermann, R. Zanetti-Dallenbach, P. Oertle, J. T. Hyotyla, U. Aebi, M. Bentires-Alj, R. Y. H. Lim and C. A. Schoenenberger, *Nat Nanotechnol*, 2012, 7, 757-765.
28. K. J. Siegrist, S. H. Reynolds, M. L. Kashon, D. T. Lowry, C. B. Dong, A. F. Hubbs, S. H. Young, J. L. Salisbury, D. W. Porter, S. A. Benkovic, M. McCawley, M. J. Keane, J. T. Mastovich, K. L. Bunker, L. G. Cena, M. C. Sparrow, J. L. Sturgeon, C. Z. Dinu and L. M. Sargent, *Part Fibre Toxicol*, 2014, 11.
29. D. Gavello, I. Fenoglio, B. Fubini, F. Cesano, F. Premoselli, A. Renna, E. Carbone and V. Carabelli, *Neurotoxicology*, 2013, 39, 84-94.
30. Z. B. Liu, X. Dong, L. P. Song, H. L. Zhang, L. X. Liu, D. W. Zhu, C. X. Song and X. G. Leng, *J Biomed Mater Res A*, 2014, 102, 665-673.
31. C. B. Dong, A. S. Campell, R. Eldawud, G. Perhinschi, Y. Rojanasakul and C. Z. Dinu, *Appl Surf Sci*, 2013, 264, 261-268.
32. S. Hirano, Y. Fujitani, A. Furuyama and S. Kanno, *Toxicol Appl Pharm*, 2010, 249, 8-15.
33. M. Asakura, T. Sasaki, T. Sugiyama, M. Takaya, S. Koda, K. Nagano, H. Arito and S. Fukushima, *J Occup Health*, 2010, 52, 9-20.
34. L. Sargent, S. Reynolds, D. Lowry, M. Kashon, S. Benkovic, J. Salisbury, A. Hubbs, M. Keane, J. Mastovich and K. Bunker, *Proc Am Assoc Cancer Res*, 2012, 53, 1320.
35. L. Rodriguez-Fernandez, R. Valiente, J. Gonzalez, J. C. Villegas and M. L. Fanarraga, *Acs Nano*, 2012, 6, 6614-6625.
36. C. Dong, R. Eldawud, L. M. Sargent, M. L. Kashon, D. Lowry, Y. Rojanasakul and C. Z. Dinu, *Environmental science. Nano*, 2014, 1, 95-603.
37. M. Foldvari and M. Bagonluri, *Nanomedicine: Nanotechnology, Biology and Medicine*, 4, 183-200.
38. A. S. Campbell, C. Dong, F. Meng, J. Hardinger, G. Perhinschi, N. Wu and C. Z. Dinu, *ACS Appl Mater Interfaces*, 2014, 6, 5393-5403.
39. A. S. Campbell, C. Dong, J. S. Dordick and C. Z. Dinu, *Process Biochemistry*, 2013, 48, 1355-1360.
40. X. C. Zhao, R. T. Liu, Z. X. Chi, Y. Teng and P. F. Qin, *J Phys Chem B*, 2010, 114, 5625-5631.
41. A. Gomes, E. Fernandes and J. L. F. C. Lima, *J Biochem Bioph Meth*, 2005, 65, 45-80.
42. C. Rotsch, K. Jacobson and M. Radmacher, *Proc Natl Acad Sci U S A*, 1999, 96, 921-926.
43. A. B. Mathur, G. A. Truskey and W. M. Reichert, *Biophys J*, 2000, 78, 1725-1735.
44. M. Radmacher, M. Fritz, C. M. Kacher, J. P. Cleveland and P. K. Hansma, *Biophys J*, 1996, 70, 556-567.
45. V. M. Laurent, S. Kasas, A. Yersin, T. E. Schaffer, S. Catsicas, G. Dietler, A. B. Verkhovsky and J. J. Meister, *Biophys J*, 2005, 89, 667-675.
46. T. G. Kuznetsova, M. N. Starodubtseva, N. I. Yegorenkov, S. A. Chizhik and R. I. Zhdanov, *Micron*, 2007, 38, 824-833.

47. B. Ohler, *Rev Sci Instrum*, 2007, 78.
48. S. Luanpitpong, L. Wang, V. Castranova and Y. Rojanasakul, *Part Fibre Toxicol*, 2014, 11, 22.
49. V. E. Kagan, Y. Y. Tyurina, V. A. Tyurin, N. V. Konduru, A. I. Potapovich, A. N. Osipov, E. R. Kisin, D. Schwegler-Berry, R. Mercer, V. Castranova and A. A. Shvedova, *Toxicology Letters*, 2006, 165, 88-100.
50. T. A. Saleh, *Appl Surf Sci*, 2011, 257, 7746-7751.
51. K. Kostarelos, L. Lacerda, G. Pastorin, W. Wu, S. Wieckowski, J. Luangsivilay, S. Godefroy, D. Pantarotto, J. P. Briand, S. Muller, M. Prato and A. Bianco, *Nat Nanotechnol*, 2007, 2, 108-113.
52. C. Z. Dinu, G. Zhu, S. S. Bale, G. Anand, P. J. Reeder, K. Sanford, G. Whited, R. S. Kane and J. S. Dordick, *Adv Funct Mater*, 2010, 20, 392-398.
53. C. Bertulli, H. J. Beeson, T. Hasan and Y. Y. Huang, *Nanotechnology*, 2013, 24, 265102.
54. B. D. Holt, K. N. Dahl and M. F. Islam, *Small*, 2011, 7, 2348-2355.
55. N. Grover, I. V. Borkar, C. Z. Dinu, R. S. Kane and J. S. Dordick, *Enzyme and Microbial Technology*, 2012, 50, 271-279.
56. S. Vardharajula, S. Z. Ali, P. M. Tiwari, E. Eroğlu, K. Vig, V. A. Dennis and S. R. Singh, *Int J Nanomed*, 2012, 7, 5361-5374.
57. A. S. Campbell, C. Dong, A. Maloney, J. Hardinger, X. Hu, F. Meng, A. Guiseppe-Elie, N. Wu and C. Z. Dinu, *Nano LIFE*, 2014, 04, 1450005.
58. J. B. Griffiths, *Dev Biol Stand*, 1987, 66, 155-160.
59. Z. Yang and H.-R. Xiong, *Culture Conditions and Types of Growth Media for Mammalian Cells*, 2012.
60. L. Bokobza and J. Zhang, *Express Polym Lett*, 2012, 6, 601-608.
61. S. N. Bokova, E. D. Obraztsova, V. V. Grebenyukov, K. V. Elumeeva, A. V. Ishchenko and V. L. Kuznetsov, *Phys Status Solidi B*, 2010, 247, 2827-2830.
62. C. S. Hu, C. H. Chiang, P. D. Hong and M. K. Yeh, *Int J Nanomed*, 2012, 7, 4861-4872.
63. S. H. Lecker, A. L. Goldberg and W. E. Mitch, *J Am Soc Nephrol*, 2006, 17, 1807-1819.
64. B. Kang, S. Chang, Y. Dai, D. Yu and D. Chen, *Small*, 2010, 6, 2362-2366.
65. D. A. Tsyboulski, J.-D. R. Rocha, S. M. Bachilo, L. Cognet and R. B. Weisman, *Nano Lett*, 2007, 7, 3080-3085.
66. L. Cognet, D. A. Tsyboulski, J.-D. R. Rocha, C. D. Doyle, J. M. Tour and R. B. Weisman, *Science*, 2007, 316, 1465-1468.
67. V. Neves, E. Heister, S. Costa, C. Tîlmaciu, E. Borowiak-Palen, C. E. Giusca, E. Flahaut, B. Soula, H. M. Coley, J. McFadden and S. R. P. Silva, *Adv Funct Mater*, 2010, 20, 3272-3279.
68. C. F. Labuschagne and A. B. Brenkman, *Ageing Research Reviews*, 2013, 12, 918-930.
69. P. Ravichandran, A. Periyakaruppan, B. Sadanandan, V. Ramesh, J. C. Hall, O. Jejelowo and G. T. Ramesh, *J Biochem Mol Toxic*, 2009, 23, 333-344.
70. M. Pacurari, Y. Qian, W. Fu, D. Schwegler-Berry, M. Ding, V. Castranova and N. L. Guo, *J Toxicol Env Heal A*, 2012, 75, 129-147.
71. A. Manke, L. Wang and Y. Rojanasakul, *Biomed Res Int*, 2013, 2013, 942916.
72. M. Pacurari, X. J. Yin, M. Ding, S. S. Leonard, D. Schwegler-Berry, B. S. Ducatman, M. Chirila, M. Endo, V. Castranova and V. Vallyathan, *Nanotoxicology*, 2008, 2, 155-170.
73. A. Manke, S. Luanpitpong, C. Dong, L. Wang, X. He, L. Battelli, R. Derk, T. A. Stueckle, D. W. Porter, T. Sager, H. Gou, C. Z. Dinu, N. Wu, R. R. Mercer and Y. Rojanasakul,

International journal of molecular sciences, 2014, 15, 7444-7461.
74. E. Eruslanov and S. Kusmartsev, *Methods in molecular biology (Clifton, N.J.)*, 2010, 594, 57-72.
75. F. Thayyullathil, S. Chathoth, A. Hago, M. Patel and S. Galadari, *Free Radical Biology and Medicine*, 2008, 45, 1403-1412.
76. P. Boldog, K. Hajdu, M. Magyar, E. Hideg, K. Hernadi, E. Horvath, A. Magrez, K. Nagy, G. Varo, L. Forro and L. Nagy, *Phys Status Solidi B*, 2013, 250, 2539-2543.
77. M. Luo, X. Y. Deng, X. Z. Shen, L. Dong and Y. F. Liu, *J Nanosci Nanotechno*, 2012, 12, 274-283.
78. Y.-Y. Guo, J. Zhang, Y.-F. Zheng, J. Yang and X.-Q. Zhu, *Mutation Research/Genetic Toxicology and Environmental Mutagenesis*, 2011, 721, 184-191.
79. I. Fenoglio, M. Tomatis, D. Lison, J. Muller, A. Fonseca, J. B. Nagy and B. Fubini, *Free Radical Biology and Medicine*, 2006, 40, 1227-1233.
80. Y. Sato, A. Yokoyama, K. Shibata, Y. Akimoto, S. Ogino, Y. Nodasaka, T. Kohgo, K. Tamura, T. Akasaka, M. Uo, K. Motomiya, B. Jeyadevan, M. Ishiguro, R. Hatakeyama, F. Watari and K. Tohji, *Molecular bioSystems*, 2005, 1, 176-182.
81. E. Aldieri, I. Fenoglio, F. Cesano, E. Gazzano, G. Gulino, D. Scarano, A. Attanasio, G. Mazzucco, D. Ghigo and B. Fubini, *Journal of toxicology and environmental health. Part A*, 2013, 76, 1056-1071.
82. K. Buyukhatipoglu and A. M. Clyne, *J Biomed Mater Res A*, 2011, 96A, 186-195.
83. F. Rico, J. Alcaraz, J. J. Fredberg and D. Navajas, *Int J Nanotechnol*, 2005, 2, 180-194.
84. J. Rheinlaender, N. A. Geisse, R. Proksch and T. E. Schaffer, *Langmuir*, 2011, 27, 697-704.
85. D. P. Juan P Ruiz, Janice Dias, Noël M Ziebarth, Herman S Cheung, *Cell Health Cytoskelet*, 2012, 4, 29-35.
86. B. D. Holt, P. A. Short, A. D. Rape, Y. L. Wang, M. F. Islam and K. N. Dahl, *Acs Nano*, 2010, 4, 4872-4878.
87. B. N. Snyder-Talkington, M. Pacurari, C. L. Dong, S. S. Leonard, D. Schwegler-Berry, V. Castranova, Y. Qian and N. L. Guo, *Toxicol Sci*, 2013, 133, 79-89.
88. I. Titushkin and M. Cho, *Biophys J*, 2009, 96, 717-728.
89. F. C. Su, C. C. Wu and S. Chien, *J Med Biol Eng*, 2011, 31, 233-244.
90. J. Galle, A. Krinner, P. Buske, D. Drasdo and M. Loeffler, *Ifmbe Proc*, 2009, 25, 185-188.
91. S. E. Cross, Y. S. Jin, J. Rao and J. K. Gimzewski, *Nat Nanotechnol*, 2007, 2, 780-783.
92. M. M. Dahm, D. E. Evans, M. K. Schubauer-Berigan, M. E. Birch and J. A. Deddens, *The Annals of occupational hygiene*, 2013, 57, 328-344.

Figure Captions:

Figure 1: (a) UV-Vis spectra of free Alexa-BSA and immobilized Alexa-BSA. The spectrum of the immobilized Alexa-BSA was obtained by subtracting the absorbance values of the MWCNTs from the ones of the Alexa-BSA-MWCNT conjugates both shown in the insert. **(b)** Raman spectra of free Alexa-BSA, MWCNTs and Alexa-BSA-MWCNT conjugates.

Figure 2: (a) Normalized FITC signal of control cells, cells exposed to MWCNTs (24 $\mu g/cm^2$), cells exposed to free Alexa-BSA, and cells exposed to Alex-BSA-MWCNT conjugates respectively at different time points. FITC signal for the Alexa-BSA or MWCNT-based conjugates was recorded using excitation at 488 nm and emission at 515 nm; at least 10000 events were contained and analyzed in the gated area. **(b)** Comparative cross-analysis of normalized FITC signal of cells treated with Alexa-BSA-MWCNT conjugates at different time points. All differences were considered statistically significant for $p^* < 0.05$.

Figure 3: Quantification of the intracellular levels of reactive oxygen species (ROS) generated upon exposure of BEAS-2B cells to 24 $\mu g/cm^2$ MWCNTs. Intracellular ROS generation was determined using the oxidation-sensitive fluorescent probe 2′,7′-dichlorofluorescein diacetate and measuring the fluorescent intensity of control and MWCNTs exposed cells at 485 excitation and 520 emission. Results are considered significant for $p^* < 0.05$

Figure 4: **(a)** Histogram of the elastic modulus distribution of a representative control cell body and its nuclear region; **(b)** Average elastic modulus of control cells and cells treated with MWCNTs (24 $\mu g/cm^2$) at different time points (whole cell body); **(c)** Average elastic modulus of nuclear regions of control cells and cells exposed to MWCNTs at different time points. Results are considered significant for $p^* < 0.05$

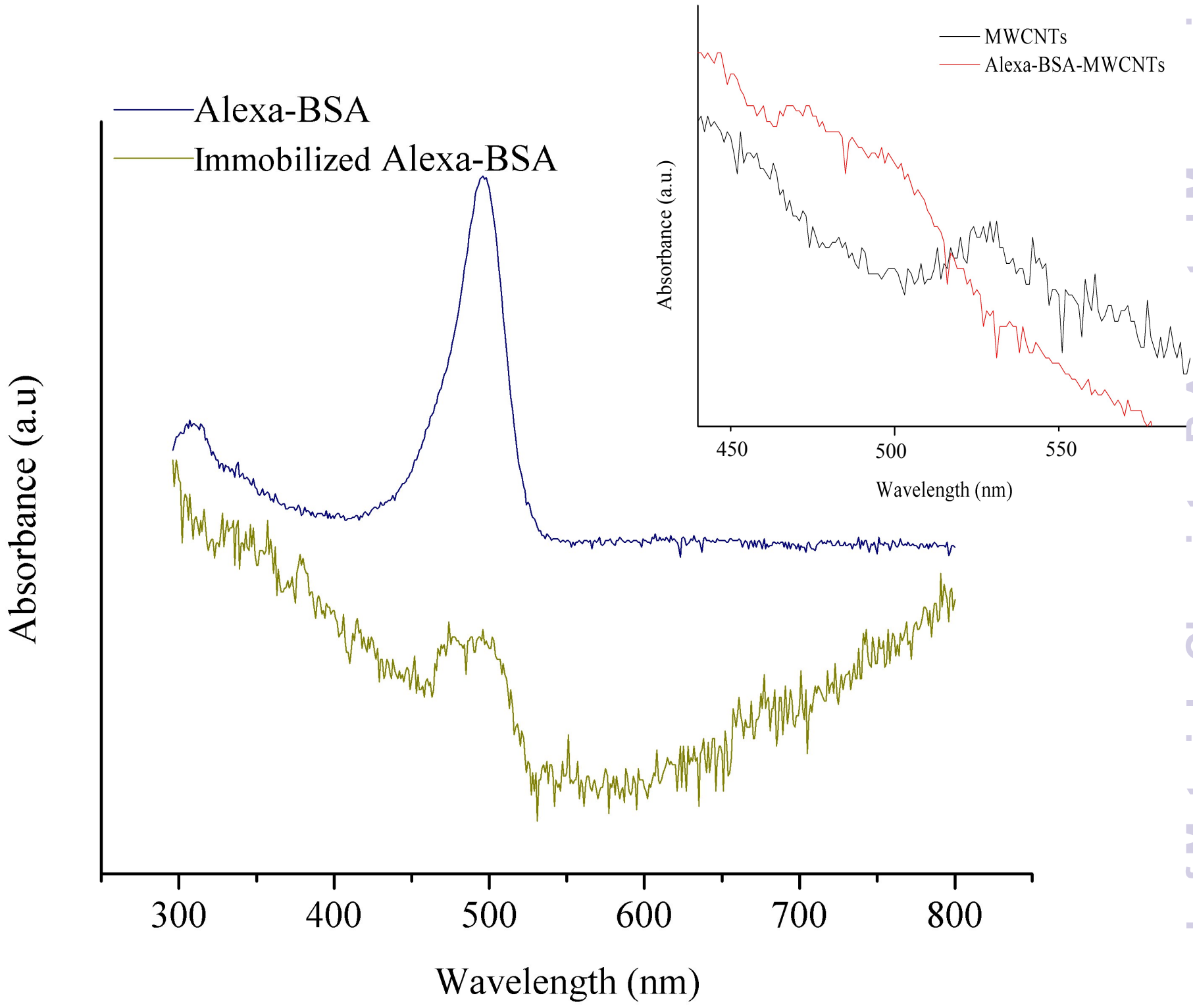

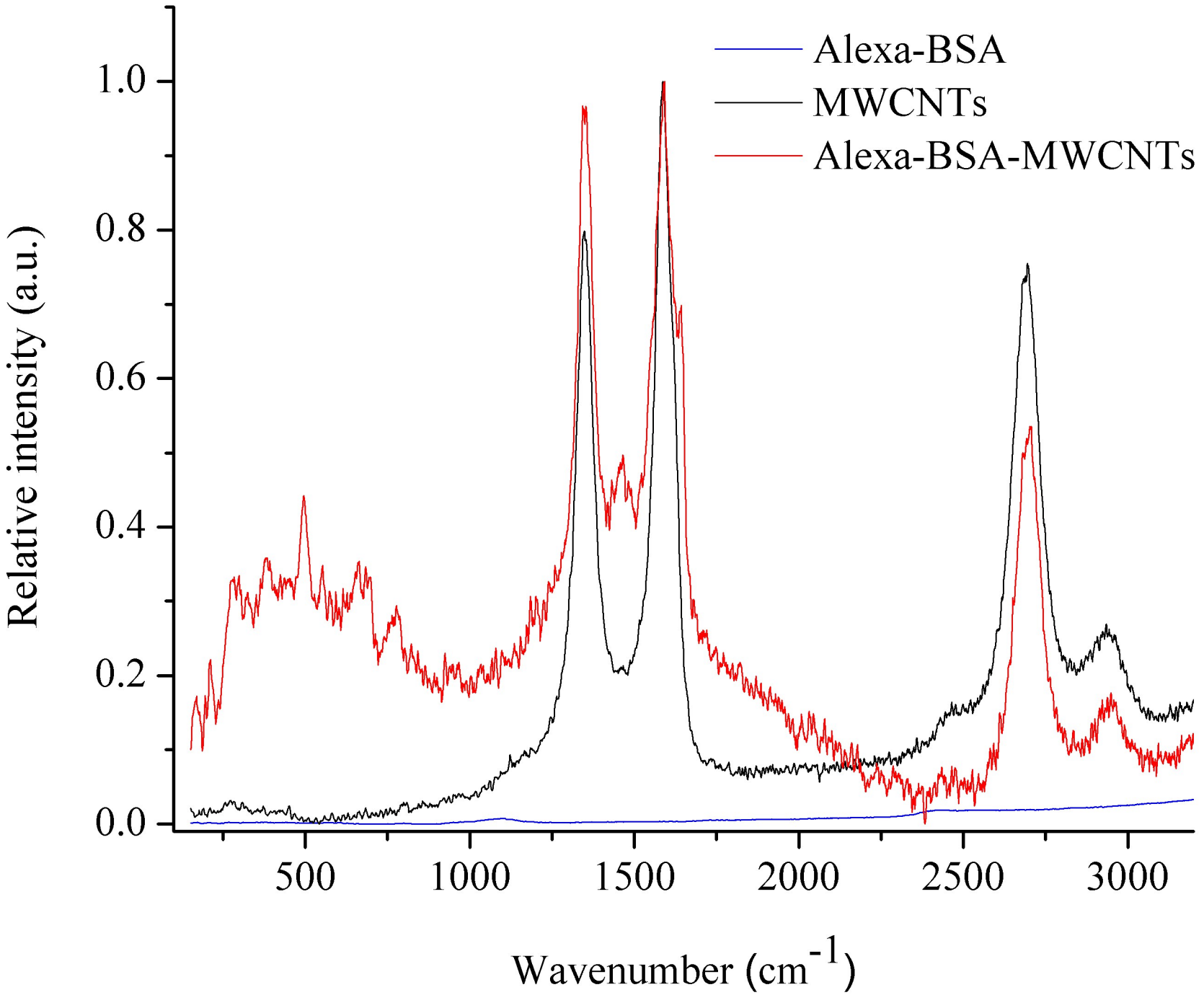

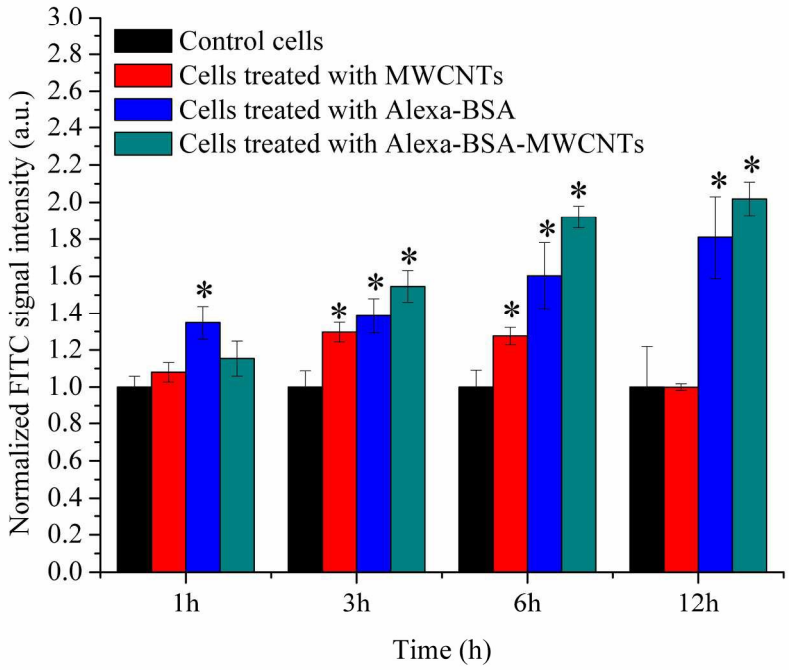

215x166mm (300 x 300 DPI)

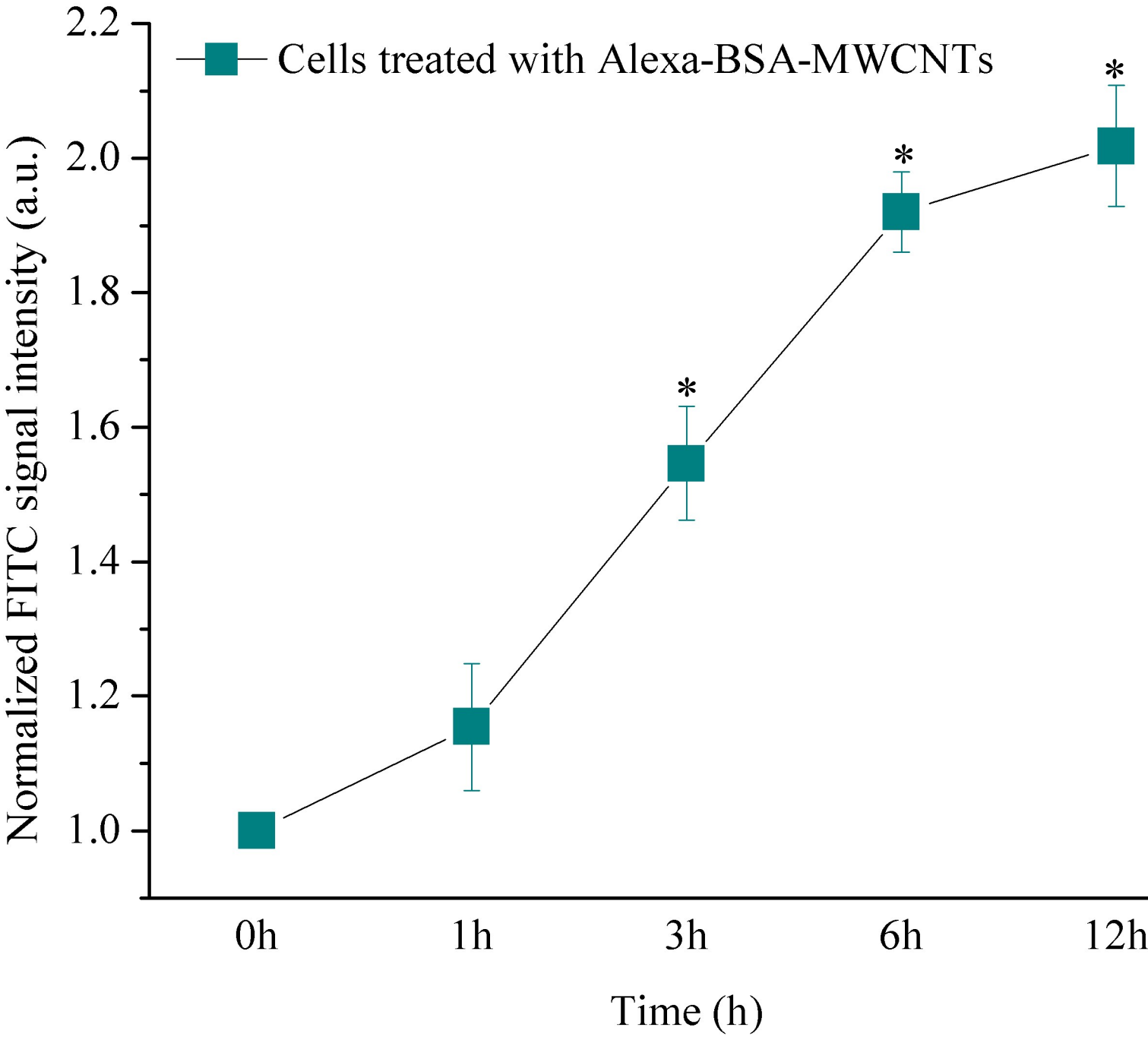

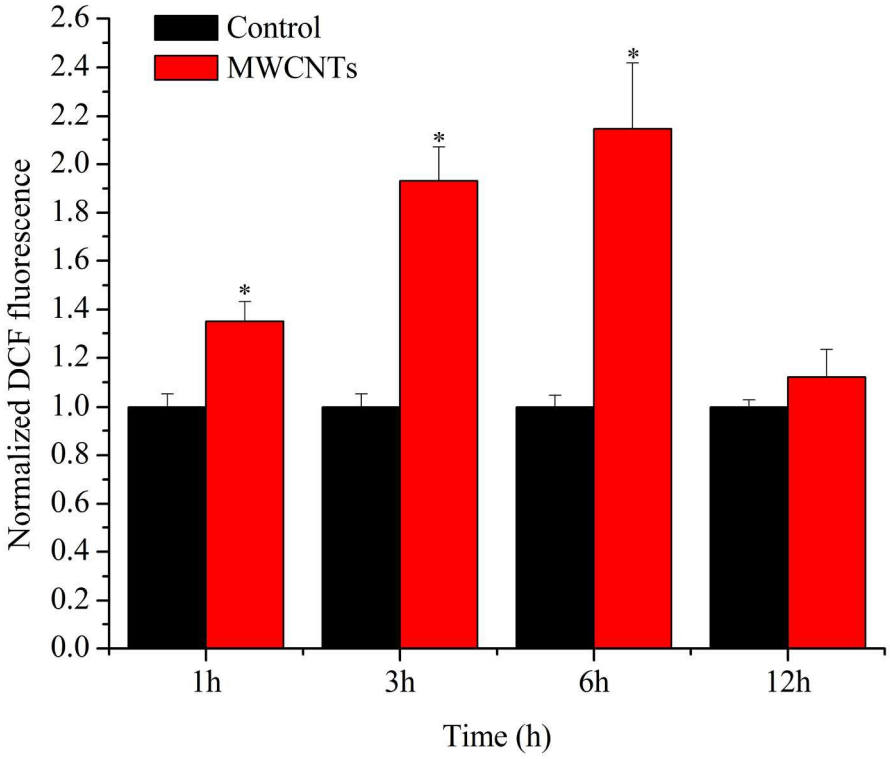

215x188mm (300 x 300 DPI)